Combustion improvement and pollutants reduction with diesel-gasoline blends by means of a highly tunable laser plasma induced ignition system

José V. Pastor, J.M. García-Oliver, A. García, C. Micó*

CMT - Motores Térmicos, Universitat Politècnica de València, Camino de Vera s/n, 46022 Valencia, Spain

*Corresponding author: Carlos Micó

e-mail: carmirec@mot.upv.es

Phone: +34 654919619

Abstract

The use of alternative fuels in compression ignition engines, either completely or partially replacing the conventional ones, have potential to reduce pollutant emissions (especially soot). However, some of these fuels do not provide good ignition features under diesel engine like conditions, which affects engine efficiency. Thus, in order to extend the application of alternative fuels, the current research proposes the use of a laser induced plasma ignition system to assist on the combustion of blends of fuels with less reactivity than pure diesel. This fuel has been chosen as the base component and it has been mixed with gasoline (as the low-reactivity fuel) in different ratios as an example of fuels with very different reactivity properties. Tests have been performed in a single cylinder optically accessible engine, allowing deeper study of combustion development and soot formation. For different in-cylinder conditions and fuel blends, the effect of laser induced plasma ignition system has been evaluated at different crank angle degrees and locations inside the combustion chamber. The application of these blends under low-reactivity engine conditions show that combustion efficiency is dramatically affected. However, the study proves that it is possible to control blend ignition delay and flame lift-off length by means of laser induced plasma. Besides, using the proper ignition system configuration, combustion characteristics similar to those of diesel fuel autoignition can be achieved for high gasoline substitution rates. They lead to similar energy release rates, which confirms that diesel-gasoline blends can reach a combustion efficiency close to pure diesel, while a strong reduction on soot formation was also obtained. These results open a door to efficiency improvement and pollutant reduction by means of a highly tunable ignition of alternative fuel blends.

Keywords: dieseline; compression ignition engine; laser plasma ignition; alternative fuel; soot reduction.

1. Introduction

Internal Combustion Engines (ICE) play a major role in our society as they represent the main road transportation powertrain mode. However, the use of any kind of fossil fuel implies pollutant emissions. For this reason, after a century of use, their footprint is undeniable. On one hand, the large particulate matter and NO_x concentrations in high-dense traffic areas, which are related with serious health issues. On the other hand, the CO_2 emissions that contribute to the green-house effect and global warming (Wang et al., 2020). In this context, new powertrain technologies have arisen during last years. The electric motor or the hydrogen fuel cell are good examples. Nevertheless, they are still more expensive solutions than ICE and require an infrastructure which hinder their short-term expansion (Hu et al., 2020). For this reason, it is mandatory that industry and researchers keep developing new solutions to minimize ICE environmental impact while improving their efficiency.

In this regard, the benefits of using alternative fuels in compression ignition (CI) engines are evident. Biofuels and bio-alcohols (Bae and Kim, 2017; Hossain and Davies, 2010), liquefied petroleum gas (LPG) (Goto et al., 1999; Jian et al., 2001) or synthetic fuels like the oxymethylene ethers (OMEx) (Liu et al., 2019; Omari et al., 2017; J.V. Pastor et al., 2020) have been the focus of many research works. Even blends of conventional fuels (e.g., dieseline) playing this role have been evaluated (Sequino et al., 2020). However, some of the most promising alternatives (e.g., oxygenated bio-alcohols) cannot be used independently due to its lower chemical reactivity or low heating value (Kumar et al., 2013; Miller Jothi et al., 2007; Rajak et al., 2020). In general, a lower reactivity results in larger ignition delays which, on one hand, improve air-fuel mixture and reduce soot formation (Pickett and Siebers, 2004). However, on the other hand, combustion efficiency could be affected and, even under certain circumstances (low temperature and low oxygen concentration), autoignition could not take place (Kim and Choi, 2008; Yilmaz et al., 2014). To overcome this drawback, alternative fuels are usually blended with conventional fuels. Nevertheless, mixture fraction is still sometimes limited and, consequently, its effects over pollutant formation and/or efficiency are reduced.

A way to extend the application of low-reactive fuels in CI engines is combining them with ignition systems, to assist and control combustion phasing. This strategy is being exploited for Low Temperature Combustion (LTC) modes (Pastor et al., 2013). In this context, conventional spark plugs have been used under wide range of engine operation conditions (Benajes et al., 2013; Triantopoulos et al., 2020). However, it is difficult to apply them in conventional diffusion combustion and not many applications can be found in this regard. In the last decade, some alternatives to electrical discharge plugs have been investigated. The microwave-assisted plasma (Hwang et al., 2017) or the laser induced plasma (LIP) are good examples. The LIP system consists on a short laser pulse, which is fired into the combustion chamber and causes air molecules to breakdown and release energy. Weinberg et al. (Felix Jiri Weinberg, 1971) first reported the capability of this technique to ignite combustible mixtures and Dale et al. (Dale et al., 1978) proved its success in internal combustion engines, even improving spark plug performance under lean mixture conditions. In the last years, the development of new combustion concepts (both SI and CI) has renewed the interest for this ignition technique (Genzale et al., 2011; Phuoc, 2006; Weinrotter et al., 2005).

In this work, a LIP ignition system has been evaluated to assist the ignition of a low-reactivity fuel (LRF) blended with diesel, in a CI engine. The main objective of the study is, on one hand, to prove that LIP is effective in facilitating the ignition of low-reactivity fuel blends under variety of engine operating conditions. On the other hand, to characterize combustion performance and soot formation of the blends under forced-ignition conditions. The laser system was developed on purpose and allows adjusting ignition timing and location inside the combustion chamber. Diesel has been chosen as base-line fuel while regular gasoline has been chosen as LRF, due to its high availability and ease of use. First, the study addresses the behavior and limitations of the different blends of gasoline and diesel to auto-ignite and burn efficiently under selected operating conditions. Then, the LIP system is applied to control combustion phasing and location, in order to improve combustion performance. For this study, three optical techniques were applied simultaneously to visualize and measure flame radiation, soot light extinction and OH* chemiluminescence. Besides, they were combined with in-cylinder thermodynamic analysis to characterize combustion process. Results confirm that, under low-reactivity operating conditions, blends with high LRF fraction do not ignite. Under these circumstances, the LIP system is able to ensure ignition. Besides, it allows controlling combustion phasing and spatial location in terms of parameters such as ignition delay or lift-off length, showing the way to efficiency improvement and pollutant reduction by means of a highly tunable ignition.

This research proves that diesel-gasoline blends, mixed out of the engine cylinder, have potential to reduce soot emissions in CI engines as long as they are combined with an ignition system as it is proposed in this work. Results presented here open a door to extend the use in CI engines of certain alternative fuels, in combination with a highly tunable ignition system, to reduce pollutant emissions without affecting engine efficiency and therefore, CO_2 emissions. The application of this strategy in the near future is probably more suited to heavy duty engines, with lower space restrictions and larger sprays, which makes control of ignition and lift-off by means of laser easier to implement. Additionally, the LIP system has shown great potential as a research tool. It allows forcing ignition characteristics and isolate them from latter soot formation. This will allow deepening in future works into the pollutant formation mechanisms related with fuel molecule structure among others.

Considering the above-mentioned, the novelty of the present work is twofold: on the one hand, the application of a LIP ignition system to assist ignition of different blend ratios of a low-reactivity fuel (LRF) under variety of CI engine-like conditions; on the other hand, the confirmation of the improvement of engine combustion of the gasoline-diesel blends with a forced ignition event, which maybe uncoupled from the fuel reactivity properties.

2. Experimental Methodology

2.1. Experimental facility

Test were performed in an optically accessible test rig, which is described in detail in (Bermúdez et al., 2003). It is based on a 2-stroke single cylinder direct injection CI engine (Jenbach JW 50), with three liter displacement and 15.7 effective compression ratio. The cylinder head was especially designed to provide four optical accesses to a cylindrical shaped combustion chamber. In this way, spray-wall interaction is avoided. Air management is handled by transfers on the liner. Thus, the cylinder head has only one port on the upper part where the injector is mounted. One of the optical accesses is used to install a pressure transducer, while the other three are equipped with oval-shaped quartz windows, 88 x 37mm and 28mm thickness. A cutaway view is presented in Figure 1.

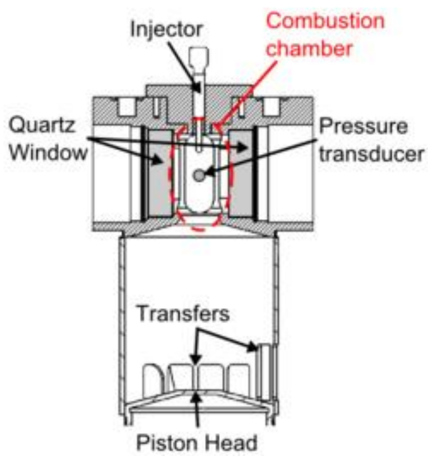

Figure 1 Cutaway view of the cylinder head layout (Pastor et al., 2016a)

In-cylinder operating conditions are controlled by means of intake air temperature and pressure. For this purpose, two sets of electrical resistors are installed at the intake line, while a root compressor is used to achieve the desired pressure. Engine is motored at 500rpm to minimize air movement within the combustion chamber and avoid disturbing spray evolution when the piston is reaching top dead center. The test rig is operated under skip-fired mode (one injection each 30 cycles), so in-cylinder thermodynamic conditions when fuel is injected are constant between different injection cycles. Besides, it ensures optical accesses integrity by reducing both thermal and mechanical stress. The cylinder head and engine block temperature is controlled by a cooling system, and the temperature is set to 353K to ensure good lubricant properties.

A conventional common-rail injection system was used, in combination with a piezoelectric injector with a single-hole 140µm diameter nozzle. The orifice was 1mm long with conical shape (Ks factor of 1.5). The fuel injected mass was low in comparison with the trapped air inside the cylinder, so thermodynamic conditions inside the combustion chamber were not affected by fuel evaporation (Nerva, 2013). Besides, thanks to the low injection rate, nozzle tip and injected fuel temperature could be considered constant between different injection cycles.

2.2. Laser induced plasma ignition system

A high-energy pulsed Nd:YAG laser (Continuum Surelite II) was used as the radiation source to induce plasma inside the combustion chamber. It was operated at 10Hz, with a maximum energy per pulse of 350mJ at 1064nm. The beam was directed into the combustion chamber by means of a periscope arrangement, which allowed to vary plasma location along the spray axis (Figure 2). An nBK-7 spherical lens, with 300mm focal length, was used to focus the beam at the spray axis. More details regarding the optical arrangement can be found at (Pastor et al., 2016b), as well as a study of the repeatability and the reliability of the LIP system.

2.3. Fuel properties

Two different diesel-gasoline blends were used in this study and compared with pure diesel, which was considered as the reference fuel. They contained 50% and 70% of gasoline in volume. They have been identified in the manuscript as “5050” and “7030” respectively, while pure diesel has been named as “B0”. Lower gasoline blend ratios showed no significant differences compared to the reference fuel, while larger gasoline ratios did not ignite under any circumstance, hindering the evaluation of the LIP contribution. Main properties of the two components are presented in Table 1.

Parameter	Gasoline	Diesel
Density at 15ºC $[kg/m^3]$	755.0	834.7
Chemical formula	$C_{6.43}H_{11.97}O_{0.21}$	$C_{15}H_{31.9}$
Lower heating value $[MJ/kg]$	41.29	42.97
Auto ignition [°C]	400	245-285
Research cetane number	-	53
Research Octane Number	103	-

Table 1 Gasoline and diesel relevant properties, obtained from (J. Pastor et al., 2017)

2.4. Operating conditions

Three different in-cylinder operating conditions were considered in this study. They have been summarized in Table 2, indicating the representative values around top dead center (TDC). An ambient density of 22.8kg/m^3 was kept constant among the three points, while temperature was varied between low temperature (780K), medium temperature (830K) and high temperature (870K). Atmospheric air was used; thus, oxygen concentration was kept at 21%. In-cylinder conditions were calculated, according to the methodology described in (Bermúdez et al., 2003). It is based on the application of a first-law of thermodynamics to the in-cylinder pressure signal, to cycles without fuel injection. It takes into account blow-by losses, heat transfer and mechanical deformations. Due to the piston movement, air temperature and density vary along the cycle and, consequently, they are not constant during the fuel injection event. However, between the start of energizing (3 CAD before TDC) and the ignition of the fuel (maximum 3 CAD after TDC), this variation is limited to 1%. Two injection pressures (1000 and 1500bar) were considered for the three in-cylinder thermodynamic conditions. These operating conditions were chosen as they can be considered as representative of conventional compression ignition engine operating conditions.

Operating Condition	Injection Pressure [bar]	Temperature [K]	Density [kg/m3]	Oxygen [%]
LT		780	22.8	21
MT	1000/1500	830	22.8	21
HT		870	22.8	21

Table 2 Summary of engine operating conditions

For all tests, 30 injections were recorded in order to obtain statistically representative results, while reducing the influence of engine operating variability. The injector energizing time was set to 3ms (9CAD) for all conditions, which results in approximately 6ms (18CAD) real injection duration, considering electrical and hydraulic delays. The injector was triggered at 3CAD before TDC (SoE). The start of injection (SoI), however, depends on the fuel type as it was reported by Dong et. al (Han et al., 2014) . The results showed that the more content in gasoline increased the delay between start of energizing and start of injection. The effect decreased with injection pressure, but it was still visible at 1000bar. For this reason, each fuel's SoI was determined based on the high-speed extinction images. This parameter has been used as the reference to compare all results.

2.5. Pressure signal analysis

The measured in-cylinder pressure was used to characterize the combustion process. The signal was registered by an AVL GU13P pressure transducer, coupled to a Kistler 5011 amplifier. The acquisition was synchronized through a flywheel magnetic encoder, providing a 6kHz sampling frequency. The pressure signal of every acquired combustion event consisted of a pair of engine cycles: the combustion cycle and the previous motored one.

This signal was used to measure ignition delay (ID). For each repetition, the combustion and motored cycle pressures were subtracted (ΔP). Then, ID was calculated as the time elapsed between SoI and the first instant when ΔP rise exceeds two times the standard deviation of a moving sampling of the ΔP signal. Additionally, the in-cylinder pressure signal was also utilized to obtain the apparent heat released (aHR) and the apparent rate of heat released (aRoHR). They were calculated by applying the first-law of thermodynamics to the cylinder volume for combustion cycles.

2.6. Optical techniques

Three optical techniques were applied simultaneously to analyze performance of LIP ignition system and its effects over soot formation: Natural Luminosity (NL), Diffused Back Illumination extinction (DBI) and OH* chemiluminescence (OH*). A sketch of the optical set-up is presented in Figure 2 . As it can be observed, two optical accesses were dedicated to DBI and NL, while the third one was used for LIP and OH*.

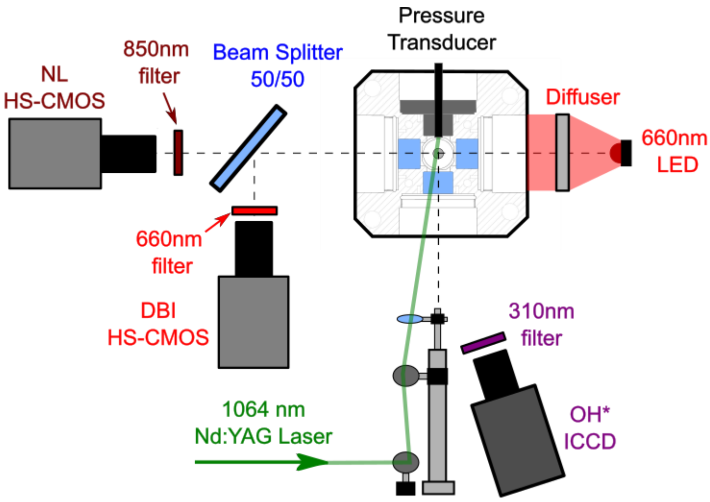

Figure 2 Sketch of the optical set-up

2.6.1. OH* chemiluminescence

The OH radicals are widely recognized as tracers of high temperature combustion zones in diffusion flames (Higgins and Siebers, 2001), where fuel and soot oxidation takes place. For this reason, they have been traditionally used to measure flame lift-off length (LOL). This parameter refers to the distance between the nozzle and the closest region where high-temperature reactions take place. It is strongly related with the later soot formation (Pickett and Siebers, 2004). These radicals emit spontaneous radiation in the UV region (280 - 350nm) and its visualization makes it possible to measure LOL. For this purpose, an Andor iStar 334T ICCD was used, equipped with a 100mm focal length f/2 UV Bernhard Halle lens. An interference filter, centered at 310nm (FWHM = 10mm), was placed in front of the camera to remove most of the flame's radiation while keeping the OH* chemiluminescence. The intensifier gating was set to 1ms, and only one image per combustion cycle was registered. This configuration was chosen in order to minimize the influence of small air-flow turbulences that appears in the combustion chamber, due to piston movement. In this way, time-integrated signal was registered and the effect of small fluctuations on the flame structure was minimized. The corresponding time interval chosen was from 760 to 1760ms aSoI. This ensured that ignition took place for all operating conditions during signal registering. Besides, in-cylinder conditions did not vary significantly due to piston movement. The optical set-up resulted in a pixel/mm ratio of 9.1 in the flame axis direction, which takes into account the misalignment between the flame and the ICCD. Image processing was done as described in (Pastor et al., 2016a). First, a background segmentation was applied based on the dynamic range of each image. Then, LOL was calculated as the average distance between the nozzle and the ten nearest pixels of the flame.

2.6.2. Natural luminosity imaging

In the visible range, most of the flame spontaneous radiation corresponds to soot thermal radiation (Pastor et al., 2016b). For this reason, flame Natural Luminosity (NL) can be used as a simple tool to obtain information about combustion evolution and soot formation. However, it is important to highlight that radiation intensity is related with both soot temperature and concentration (Pastor et al., 2016a). Besides, NL includes minor contributions of chemiluminescence too, which could be relevant in low sooting flames. For this reason, care must be taken when interpreting results and its application is usually limited to qualitative analysis.

To register NL signal, a high-speed Fastcam Photron SA-5 CMOS camera was used. It was equipped with a 100mm focal length and f/2 lens, resulting in a pixel/mm ratio of 11. As it will be described below, a 660nm LED was employed for DBI measurements. Therefore, in order to avoid crosstalk between the NL signal and the LED, an interference filter centered at 850nm (FWHM = 40 nm) was installed in front of the high-speed camera. The detector was set to record at 25kHz sampling rate and 40µs exposure time. Additionally, a 50% transmission beam splitter was placed in front of the camera to direct half of the light coming from the engine to the DBI detector.

2.6.3. Diffused back-illumination extinction imaging

Diffused back-illumination (DBI) extinction imaging was applied in this study to analyze soot formation within the flame. The technique is based on measuring the light attenuation caused by soot particles, which can be related with their optical properties by means of Lambert-Beer's law, as described in Equation (1) (J.V. Pastor et al., 2015). A LED light source with an emission spectrum centered at 660nm was used to create a high-power pulsed illumination. It was combined with a diffuser to create a diffused Lambertian intensity profile (Westlye et al., 2017). At the other side of the cylinder head (Figure 2), the LED radiation was directed by a 50% reflection beam splitter towards the detector. In this work, a high-speed Photron Fastcam SA-X2 CMOS camera was used, equipped with a 100mm focal length and f/2 lens. It was set to acquire at 25kHz with an exposure time of 0.29µs.

The light arriving to the detector corresponds to the LED light source together with soot radiation. For this reason, an interference filter centered at 660nm (FWHM = 10nm) was placed in front of the detector to minimize crosstalk between both light sources. However, thermal radiation at this wavelength is still intense and DBI measurements could be biased. To solve this, the flashing frequency of the LED was set as half of the camera acquisition rate to capture a flame radiation image between every two LED pulses. Then flame luminosity could be quantified to correct the LED signal. According to the Lambert-Beer's law, the soot optical thickness (KL) was calculated as:

$$\frac{I-I_f}{I_0} = \exp\left(-KL\right) \quad (1)$$

Where I refers to the sum of the transmitted LED light and flame radiation at 660nm. I_f is the flame radiation, registered when the LED is off. I_0 is the LED reference intensity, measured before the start of injection. The product KL represents the accumulated soot extinction along the light path, which is related with the soot concentration (Tiemin Xuan et al., 2019). In this work, analysis has been done based on this parameter.

3. Results and discussion

Experimental results are presented and discussed as follows: first, a summarized analysis of the autoignition behavior of the blends has been presented to identify their operating limits; then, the capabilities and contributions of the LIP ignition system to assist fuel ignition have been detailed; finally, the effects of LIP ignition assistance over combustion development and soot formation have been described.

3.1. Autoignition

In Table 3, the effectiveness of the 7030 blend to auto-ignite under the different operating conditions considered in this work is summarized. It was calculated as the percentage of cycles in which autoignition took place out of 30 injections. As it can be observed, under LT conditions, this fuel is not reaching 100% effectiveness. Besides, it decreases as injection pressure increases. Results corresponding to B0 and 5050 haven't been included as it was 100% for all the cases. Misfiring of similar blends (gasoline-biodiesel) in CI engines, at in-cylinder temperatures around 780K, has been already reported in the literature (Vu et al., 2019).

Injection Pressure [bar]	LT	MT	HT
1000	13%	100%	100%
1500	7%	100%	100%

Table 3 Autoignition effectiveness for 7030 blend

Based on the effectiveness data, one could state that the LIP ignition system should be used under unfavorable operating conditions where blends do not auto-ignite. However, the ignition delay is another aspect that must be considered. The flame natural luminosity evolution for B0 and the two blends, at MT operating conditions and 1000bar injection pressure is presented in Figure 3. A simple analysis indicates a different ID between the three fuels. The first frame (at 2160µs aSoI) of the sequence shows that combustion already started for B0 but not for 5050 or 7030. Additionally, when comparing both blends, it is possible to see that visible radiation appears later in the cycle when increasing the gasoline fraction. This behavior confirms that this fuel is delaying the blend autoignition. When comparing B0 (reference) with the two blends for all the operating conditions (Figure 4), both 5050 and 7030 present higher ID values. As the gasoline fraction increases, the blend reactivity decreases (AlAbbad et al., 2019; Vu et al., 2019; Wang et al., 2015).

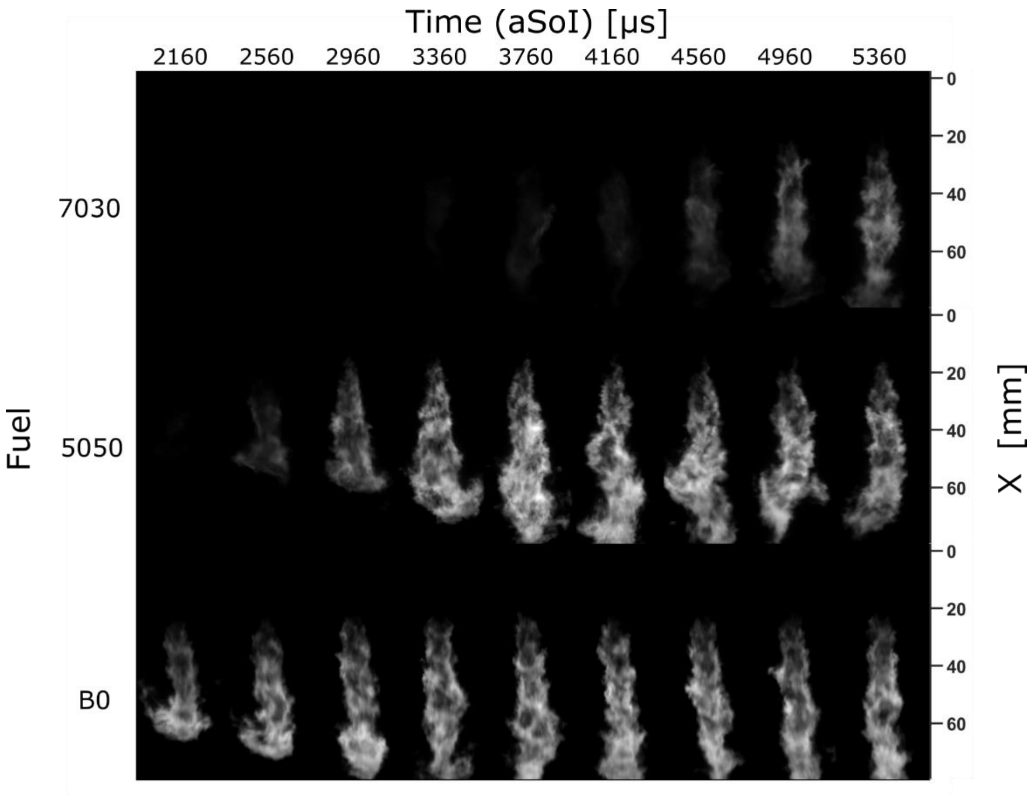

Figure 3 Flame natural luminosity sequence for B0 and the two blends, at MT operating conditions and 1000bar injection pressure without LIP ignition assistance. Images correspond to single injection events.

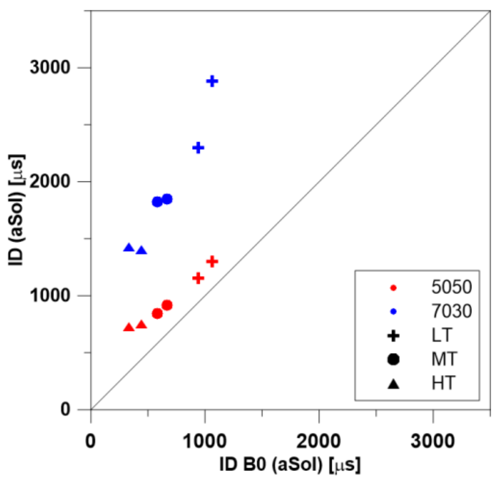

Figure 4 Ignition delay corresponding to 5050 and 7030 autoignition, compared to B0, for all operating conditions

The later ignition of 5050 and 7030 affects combustion development and energy release. In Figure 5, the aRoHR (left) and aHR (right) for B0 and 7030 at LT, MT and HT operating conditions and 1000bar injection pressure are shown. Results corresponding to 5050 and 1500bar have not been included for more clarity of the figure. As it could be expected, the accumulated energy released (aHR) is strongly affected by ID. A more delayed start of combustion causes a shorter combustion duration but also a lower RoHR. This is especially observable when comparing B0 and 7030 at LT conditions.

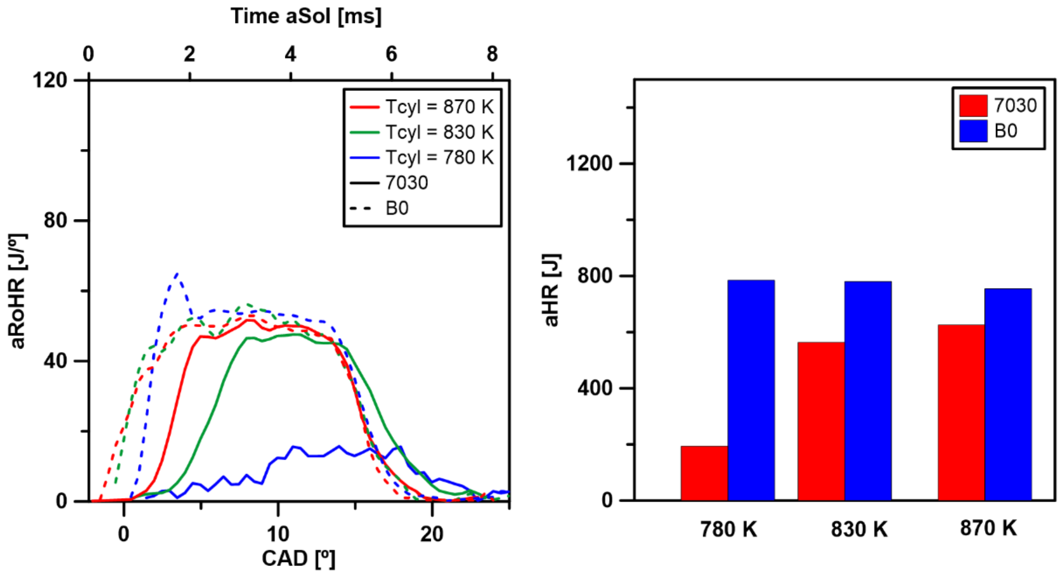

Figure 5 Apparent Rate of Heat Release (left) and apparent Heat Released (right) for B0 and 7030 autoignition combustion, at 1000bar injection pressure.

3.2. Laser induced plasma ignition

According to the above mentioned, the lower reactivity of gasoline causes larger ignition delays and affects combustion and energy release. Worst-case scenario, even under certain conditions, autoignition of the 7030 blend does not take place. In these circumstances, the application of an “external” ignition system seems justified. According to previous studies published by Pastor et al. (J. V. Pastor et al., 2017), timing and location of the LIP define the ignition delay and the lift-off length of the resulting combustion. It means that not only a proper ignition and combustion phasing could be achieved, but also soot formation could be influenced by means of the flame’s LOL.

In order to identify a proper configuration of the LIP ignition system, a sweep of both LIP timing and location was performed for 5050 and 7030 blends. B0 autoignition has been considered as a reference for this study and, for this reason, no LIP ignition tests were carried out with this fuel. Table 4 summarizes the different LIP configurations evaluated. The locations are defined as the distance to the nozzle along the spray axis, and delays are measured from SoI. They were chosen taking into account that the system does not work properly under high fuel/air ratios (close to the nozzle) (J. V. Pastor et al., 2017) and how the spray penetrates in the combustion chamber. This was previously characterized by Pastor et al. (J. Pastor et al., 2017) for the same operating conditions and hardware used in this work. It must be noted that LIP position sweep for 7030 at LT operating conditions has not been included in this work, due to experimental issues found during analysis. In this case, only LIP at 22.5mm is reported. For most of the LIP configurations tested, 100% ignition efficiency was achieved. Only at 42.5 mm from nozzle, LIP effectiveness was almost 0 for both fuels. In this case, plasma was generated at the tip of the spray. Even, for some repetitions, the spray did not reach that distance when the laser was fired. For this reason no results related with this configuration have been presented in this work.

LIP distance [mm]		15	17.5	22.5	32.5	42.5
LIP delay (aSoI) [µs]	160			X		
	560	X	X	X	X	X
	960			X		

1360	X

Table 4 Summary of LIP system configurations evaluated in this work

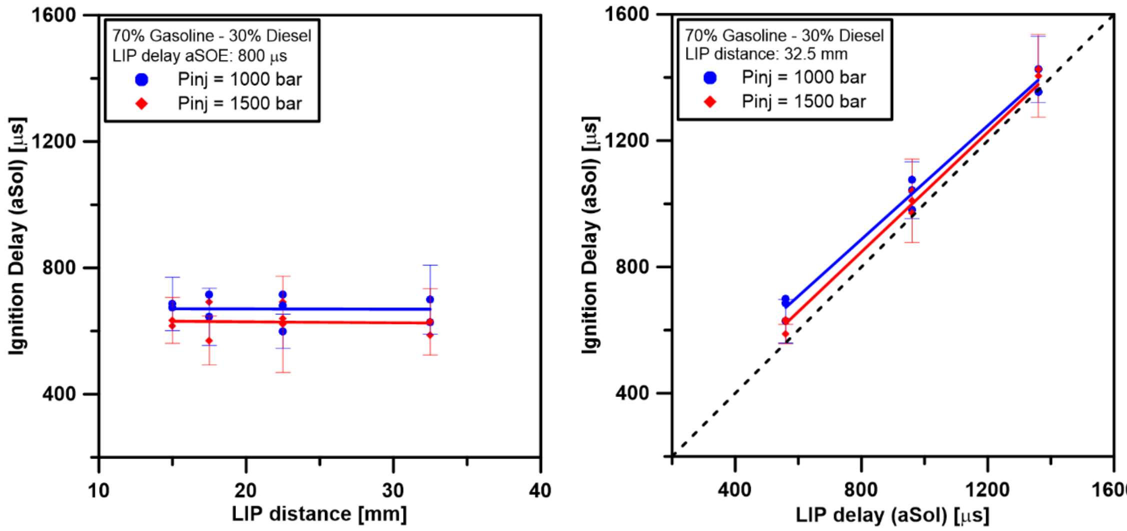

Figure 6 Effect of LIP distance (left) and LIP delay (right) over Ignition delay for 7030 at 1000 (blue) and 1500bar (red) injection pressure.

In Figure 6 the effect of LIP location (left) and delay (right) over ID is reported for 7030. Results correspond to 1000 and 1500bar at the three operating conditions. As it can be observed, the parameter that controls ignition delay is the LIP delay. As it increases, ID rises in the same proportion. In general, ignition takes place between 10 to 100μs after plasma is induced. In contrast, LIP distance shows no influence. When moving downstream the nozzle, plasma is induced under different air/fuel ratios. Thus, results suggest that the mechanisms triggered by the LIP progress with the same efficiency for a wide range of fuel concentration values. Additionally, it must be highlighted that, out of the range of LIP locations chosen for this study, the LIP system did not trigger ignition at all and no progressive transition was observed from effective to non-effective ignition system. Regarding operating conditions, there is no noticeable effect over the LIP induced ignition delay.

When evaluating flame lift-off length, the effect of LIP configuration is the opposite as the one reported for ignition delay. In Figure 7, the effect of LIP location (left) and LIP delay (right) over LOL for 7030 is shown. Results correspond to 1000 and 1500bar, at MT and HT operating conditions. In this case, an influence of the ignition system is observed when increasing the distance between the LIP and the nozzle. However, the effect of injection pressure upon LOL, which is usually observable when autoignition takes place, seems to be absent. No significant differences were detected between 1000 and 1500bar in comparison with the standard deviation of measurements (error bars). In general, it can be observed that LOL stabilizes downstream the LIP distance. However, in contrast with the ID, in this case operating conditions play an important role. When in-cylinder temperature increases, the induced LOL decreases and so it does the gap with LIP as ignition is taking place in a more reactive environment (Pickett and Siebers, 2004).

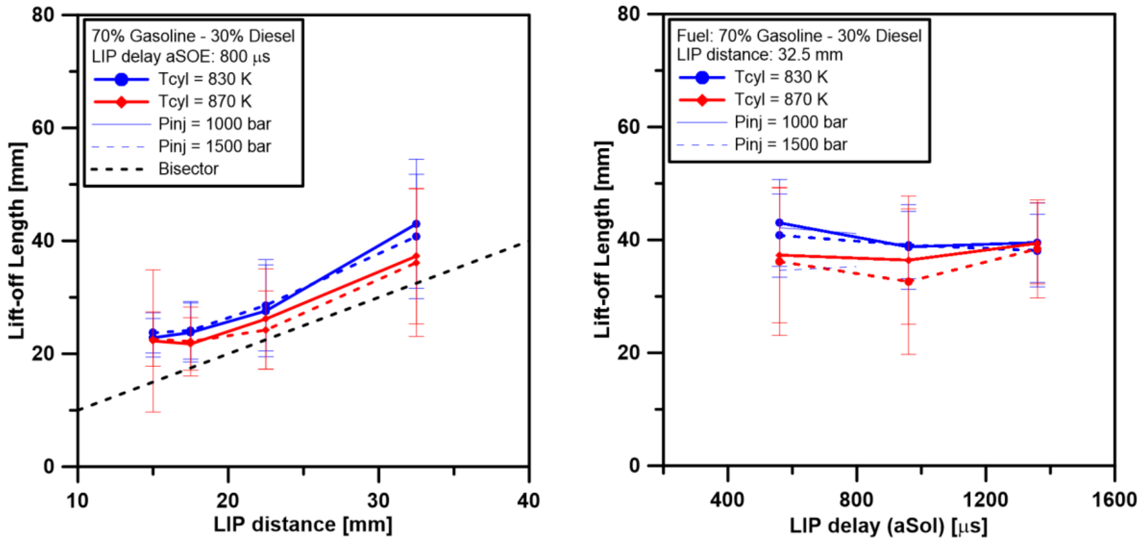

Figure 7 Effect of LIP distance (left) and LIP delay (right) over lift-off length for 7030 at MT (blue) and HT (red) operating conditions, with 1000 (continuous line) and 1500bar (dashed line) injection pressure.

The LIP configuration effect was also evaluated for 5050. In this case, the behavior observed regarding induced ID and LOL was similar to the one reported for 7030.

3.3. Laser induced plasma assisted combustion

The evaluation of different LIP positions and delays for both blends allowed to identify several configurations which provided similar ID and LOL values to those obtained for B0 autoignition. They have been summarized in Table 5, where results obtained for the two blends and B0 at 1000bar injection pressure are compared. The same configurations were chosen for 1500bar.

	7030				5050				B0	
	LIP distance [mm]	**LOL [mm]**	**LIP delay [µs]**	**ID [µs]**	**LIP distance [mm]**	**LOL [mm]**	**LIP delay [µs]**	**ID [µs]**	**LOL [mm]**	**ID [µs]**
LT	22.5	29.2	960	1076	17.5	23.6	960	984.1	29.7	1021
MT	17.5	23.8	560	715.6	17.5	25.5	260	609.43	22.6	626.6
HT	17.5	21.7	560	645	17.5	24.0	260	587.71	21.7	404.38

Table 5 LIP configurations chosen for 7030 and 5050 and the corresponding LOL and ID values, in comparison to the ones obtained for B0. Results correspond to 1000bar injection pressure.

Based on the LIP configurations of Table 5, an analysis of the influence of LIP ignition system on 5050 and 7030 combustion process has been carried out. Results are compared with those obtained for B0 autoignition, as reference. The new combustion evolution is represented in Figure 8, where natural luminosity of B0 and the two blends is presented. Images correspond to MT operating condition and 1000bar injection pressure. In comparison with Figure 3, the new NL images confirm the reduction of ID for 5050 and 7030 blends. In both cases, plasma was generated at 560µs aSoI when B0 did not ignite yet. The LIP can be observed as a small white dot, upstream the later stabilized flame LOL. At 960µs, NL is visible for the three fuels which confirms the start of combustion. The later flame evolution of B0 and the two blends is very similar.

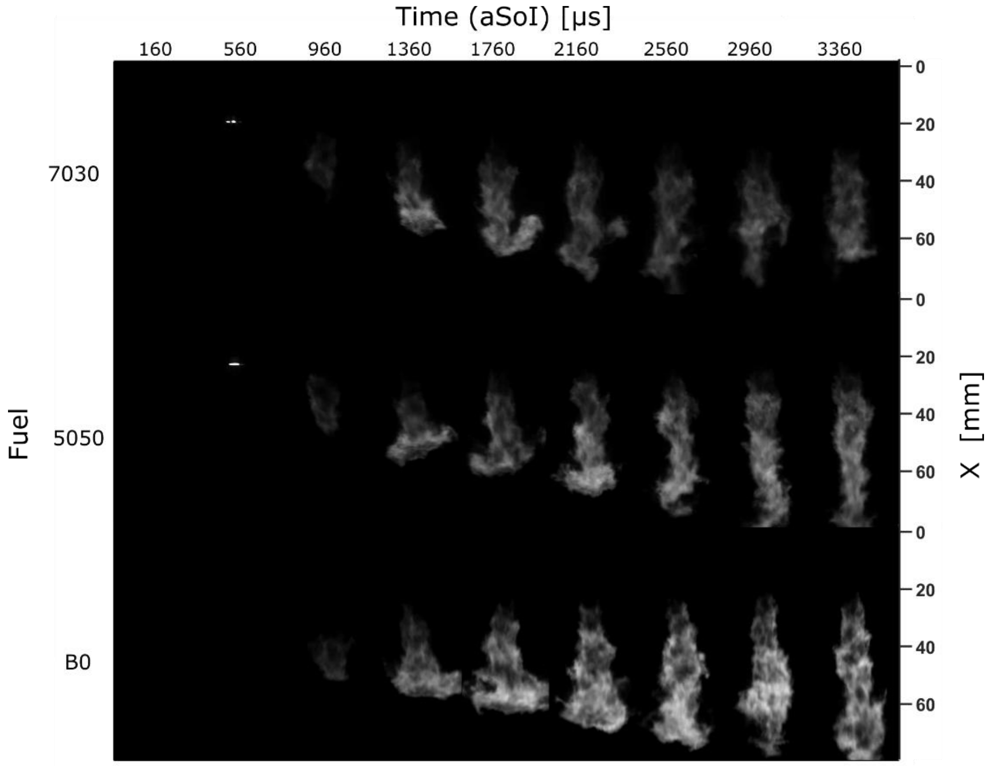

Figure 8 Flame natural luminosity sequence for B0 and the two blends, acquired at MT operating conditions and 1000bar injection pressure with LIP ignition assistance. Images correspond to single injection events.

The Figure 9 shows the aRoHR for the three fuels at all operating conditions. The first thing that must be highlighted is that, in contrast with Figure 5, differences between B0 and the two blends have been minimized. This proves the benefits of using an ignition system like the one proposed in this paper, in combination with less reactive fuels like diesel-gasoline blends. At the stabilized stage, in average, B0 RoHR is 15.4% higher than 7030 and only 6.7% than 5050 for 1000bar injection pressure. However, it is important to highlight that these differences decrease when increasing in-cylinder temperature.

This is especially noticeable when considering 1500bar cases, where B0 aRoHR is only 5% higher than 7030 and 2% than 5050.

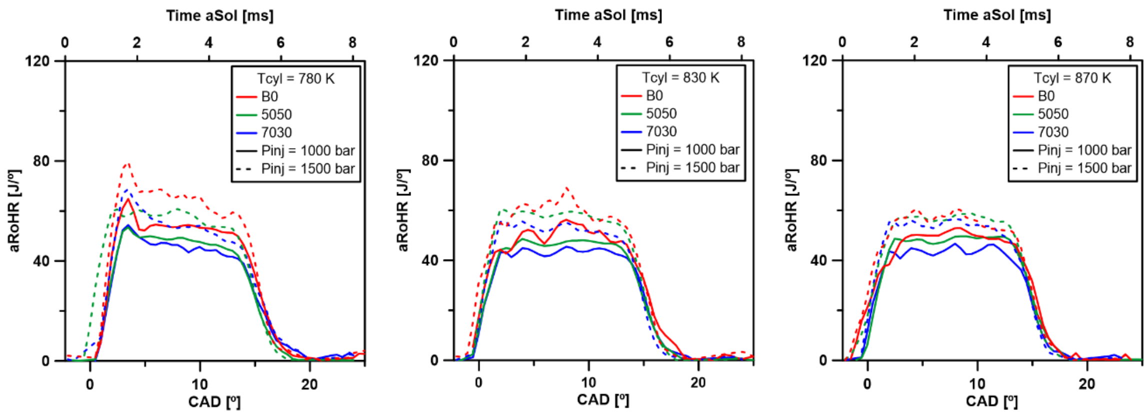

Figure 9 Apparent Rate of Heat Release for B0 and the two blends at LT (left), MT (center) and HT (right) operating conditions and 1000 (continuous line) and 1500bar (dashed line) injection pressure.

According to results obtained (Figure 9), it can be stated that the more content in gasoline, the lower the RoHR obtained. As the aRoHR for diffusive combustion is controlled by injection characteristics, differences among fuels in nozzle flow could be hypothesized as a potential explanation for the reported trend. This can be related with the different physical properties between gasoline and diesel. Pastor et al. (J. Pastor et al., 2017) analyze the hydraulic behavior of a similar injection system for different substitution rates in diesel-gasoline blends. They reported that, when gasoline fraction increases at constant injection pressure, the amount of fuel injected decreases. On the other hand, as presented in Table 1, diesel has a higher heating value. All in all, increasing the gasoline fraction results in less energy available inside the combustion chamber. In order to validate this hypothesis, an estimation of aRoHR differences between B0 and each blend have been calculated. Based on experimentally measured mass-flow rate (J. Pastor et al., 2017) and the corresponding Lower Heating Value, the theoretical aRoHR $(\dot{m}f \cdot H_c)$ for each blend was calculated and compared with B0.

Results show differences of 6% for 7030 and 5% for 5050 during the diffusion stage, which are smaller than the ones experimentally obtained. This conclusion, together with the fact that differences get reduced as in-cylinder temperature increases, suggest that the combustion process could be affected by the fuel composition. For example, not all the fuel is consumed under certain operating conditions. However, in order to confirm this hypothesis further investigation will be necessary.

The apparent Heat Released (aHR) for B0 and the two blends is summarized in Figure 10, in terms of accumulated values. The same trends as the ones described by the aRoHR are observed when quantifying the total amount of energy released during the combustion cycle. As the gasoline fraction increases the energy released decreases, despite obtaining similar combustion phasing thanks to the LIP ignition system.

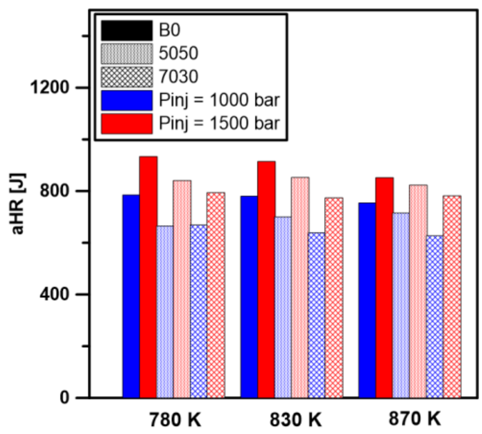

Figure 10 Apparent Heat Released for B0 and the two blends, at LT (left), MT (center) and HT (right) operating conditions and 1000 (continuous line) and 1500bar (dashed line) injection pressure.

Results prove the potential of LIP to assist ignition of less reactive fuels, as the diesel-gasoline blends, injected at variety of in-cylinder operating conditions. Focusing in LT, LIP improved ignition effectiveness to 100%, providing a more stable combustion and an aRoHR similar to the one obtained when using B0. However, it must be highlighted that not only ID but also LOL of both blends was modified in comparison with their autoignition values. In this sense, the new LOL is shorter than the original one and its effect over soot formation is unavoidable (José V. Pastor et al., 2020; Pickett and Siebers, 2004). Previous studies, where soot formation of diesel-gasoline blends was addressed, showed that an increase of gasoline faction reduced soot emissions (Benajes et al., 2017; Vu et al., 2019; Zheng et al., 2015). However, this is a reasonable behavior as the lower reactivity of this fuel increases both ID and LOL. In this work, thanks to the LIP ignition system, both parameters were kept constant despite the content in gasoline of the blends. Thus, the influence of the amount of air entrained by the fuel spray over later soot formation was almost eliminated from the analysis and the soot tendency of each fuel is highlighted.

In-cylinder soot formation was measured by means of DBI imaging. In Figure 11, soot average KL distribution for B0 and the two blends is presented. Images correspond to MT operating conditions and 1000bar injection pressure. As it can be observed, despite forcing similar LOL for 5050 and 7030 in comparison to B0, still some differences are observable. Mixing diesel and gasoline reduces soot formation in comparison with burning pure diesel.

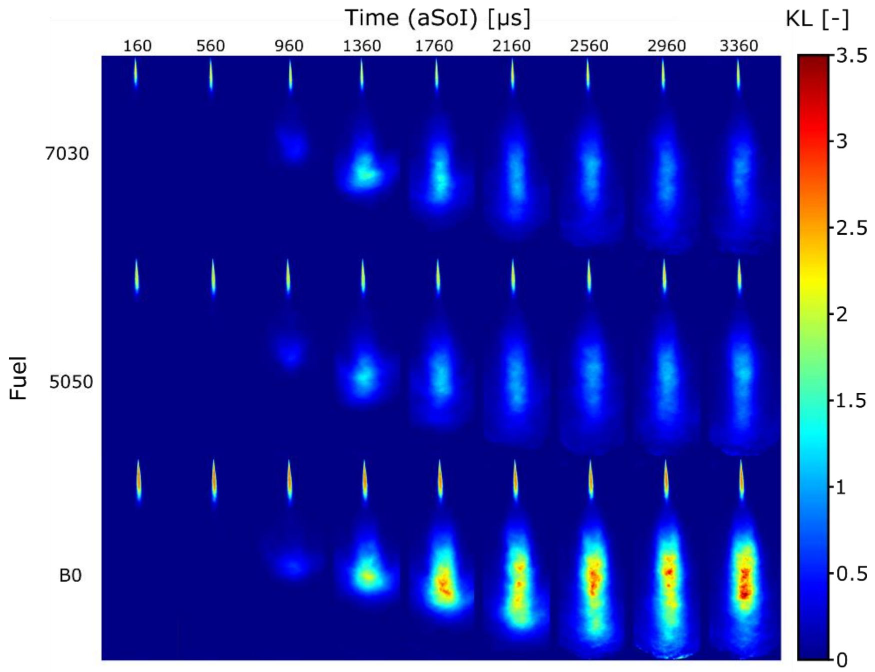

Figure 11 Soot average KL distribution sequence for B0 and the two blends, acquired at MT operating conditions and 1000 bar injection pressure with LIP ignition assistance.

In order to confirm the effect of gasoline at all operating conditions, soot average KL maps are shown in Figure 12 (P_{inj} = 1000bar) and Figure 13 (P_{inj} = 1500bar). Similar representation format has been previously used by other authors (Bakker et al., 2017; T. Xuan et al., 2019). Every DBI frame was reduced to a one-dimensional vector, containing the average KL value of all its rows (considering images as two-dimensional matrices). It represents the average KL evolution along the flame axis. Then, all these vectors were assembled consecutively to obtain maps where the vertical axis represents the distance to the nozzle and the horizontal axis represents the time aSoI of each point represented. Thus, each map provides a complete combustion sequence like the ones shown in Figure 11. In both figures, maps were organized by operating condition (columns) and fuel type (rows). Additionally, the fuel-air equivalence ratio at LOL (ϕ_{LOL}) has been estimated and included in the figure for better interpretation of results. A scaling law based on turbulent mixing considerations has been used (Pastor et al., 2008), which allows to represent the fuel mass fraction along the spray axis (Y_f) as follows:

$$Y_f = \frac{K \cdot (d_0 \cdot \sqrt{\frac{\rho_f}{\rho_a}})}{X} \qquad (2)$$

Where X is the distance to the nozzle and K is a spray constant. The term in brackets represents equivalent diameter, which depends on the nozzle outlet diameter (d_0), the fuel density (ρ_f) and the ambient density (ρ_a). A one dimensional model proposed by Pastor et al. (J. V. Pastor et al., 2015) was used to obtain the K value, which can be considered independent of fuel composition. Calculations were carried out for 7030 at MT operating conditions and both injection pressures. Then, an expression like equation (2) was fitted to the fuel mass fraction distribution at spray axis, from which K was derived. Iso-octane and hexadecane where used as gasoline and diesel surrogates. Information regarding mass flow rate and spray geometry used as input of the model was obtained from (J. Pastor et al., 2017). Finally, the fuel-air equivalence ratio at LOL was calculated based on the fuel mass fraction at LOL for each fuel and operating condition.

In Figure 12, a similar relation between gasoline content and soot formation to the one reported previously can be observed. Focusing on the ϕ_{LOL}, it can be seen that the LIP configurations chosen force ignition under leaner mixture conditions for 7030 in comparison to B0, for all operating conditions. However, this was not achieved for 5050, which at LT and HT shows higher ϕ_{LOL} than diesel. According to the literature, lower fuel-air equivalence ratio at LOL leads to less soot formation (Pickett and Siebers, 2004), which is coherent with what can be observed when comparing 7030 and B0. However, when the reference fuel is compared with 5050, this trend is not visible. Under HT operating conditions, B0 shows higher KL values despite igniting under “leaner” mixture conditions at LOL than 5050. At LT operating conditions, soot formation of both fuels is similar but it must be noted that ϕ_{LOL} is much higher for 5050 than for B0. According to this, it can be stated that fuel composition is playing a major role in soot formation, compensating the differences in terms of mixture formation at LOL. Thus, the addition of gasoline to the blend seems to reduce soot formation.

In Figure 13, results corresponding to 1500bar injection pressure are presented. Similar conclusions to the ones reported for the previous figure can be also applied here. The effect of the gasoline fraction is clear, especially when considering the differences in terms of ϕ_{LOL} between fuels. Major differences are observable when comparing B0 with the two blends. However, they are not so clear when comparing 5050 and 7030. The different ϕ_{LOL} obtained for each blend, due to the LIP configuration chosen, softens the expected trend related with fuel composition.

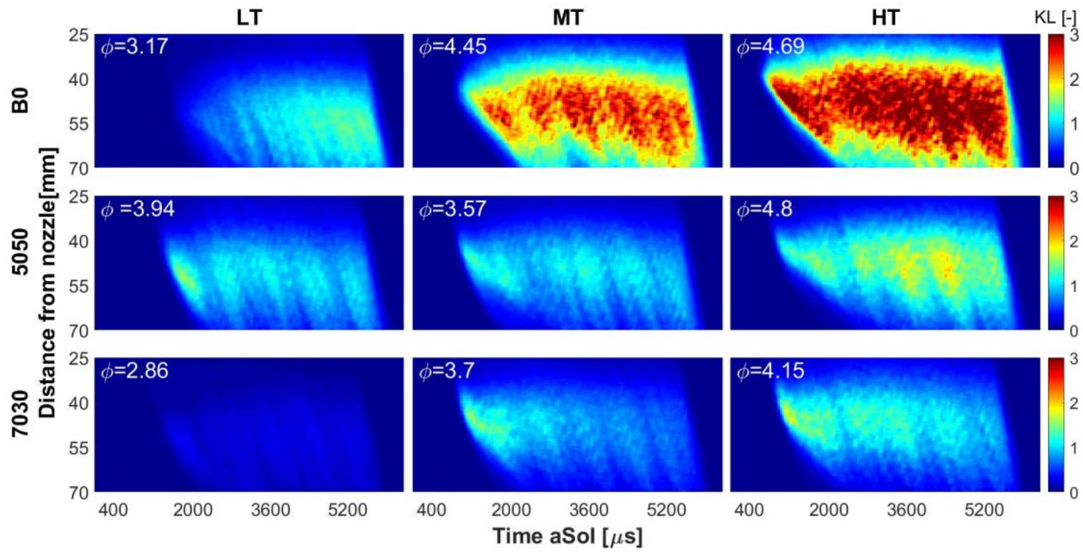

Figure 12 Soot average KL maps for B0 and the two blends, at LT (left), MT (center) and HT (right) operating conditions. Data corresponds to 1000 bar injection pressure.

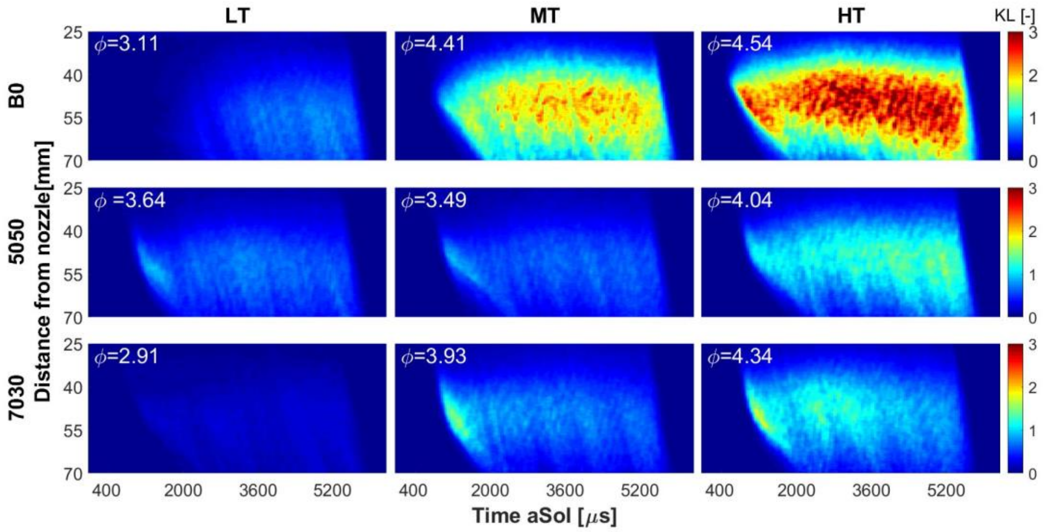

Figure 13 Soot average KL maps for B0 and the two blends, at LT (left), MT (center) and HT (right) operating conditions. Data corresponds to 1500bar injection pressure.

The soot formation tendency of a fuel has been related in the past with both its physical and chemical properties. However, the LIP system allowed to minimize the influence of the first ones. Thus, differences in chemical properties must be playing a major role. In this regard, the fuel Smoke Point (SP) and other related parameters, like the Threshold Sooting Index (TSI), have been used in numerous works to characterize the soot tendency of fuels in relation to their chemical structure. The lower the SP value, the larger the TSI and the soot tendency. In contrast with the analysis presented in this work, several studies can be found in literature where results based on SP measurements suggest that an increase of gasoline in diesel-gasoline blends should cause also an increase of the soot tendency (Gómez et al., 2020; Liu et al., 2018). However, Gómez et al. (Gómez et al., 2020) compare these measurements with a new parameter, known as Oxygen Extended Sooting Index (OESI). It was firstly proposed by Barrientos et al. (Barrientos et al., 2013) and considers the molar stoichiometric oxygen-fuel ratio of the fuel instead of its molecular weight (like TSI). For this reason, it is a more appropriate sooting index for oxygenated fuels, but it is also suitable for non-oxygenated compounds. Based on OESI, this author reports a reduction in soot tendency when the gasoline fraction increases in diesel-gasoline blends, which is coherent with the results presented in Figure 12 and Figure 13.This suggest that the less oxygen required for the fuel to oxidize when increasing gasoline content also reduces soot formation, despite reaching similar or even higher fuel-air equivalence ratio at LOL.

3.4. LIP ignition system and cleaner energy production

The LIP ignition system has been proved as a powerful tool to assist low-reactivity fuel ignition when operating conditions are unfavorable. This open a path to a greater development of alternative fuel applications for a pollutant emission reduction. Nevertheless, the possibilities of this technology are strongly related to the development of "clean" fuels.

An improvement in terms of particle matter reduction can be achieved with the ignition system either by improving combustion characteristics or by its combination with alternative fuels that promote lower in-cylinder soot formation. However, regarding CO_2 emissions reduction, the LIP ignition system contribution is limited by the properties of the fuel used. In a scenario where carbon-based fuels, with similar molecular structure (C/H ratio) and lower heat value to fossil fuels, LIP allows to reach a similar combustion efficiency. Therefore, a minimum CO_2 emission reduction could be expected.

In this regard, the lifecycle carbon footprint of alternative fuels plays a major role. The LIP ignition system allows using more sustainable fuels, which properties where not suitable to provide efficient and stable ICE operating conditions. One example are biofuels (bioalcohols). Different studies can be found in the literature which prove a reduction in CO_2 footprint when these fuels are used for energy production (Yan et al., 2020). However, the source and the process of obtaining the fuel could have a major impact on the resulting greenhouse gas emissions (Ahmed and Sarkar, 2018)(Medeiros et al., 2015).

An alternative that is gaining relevance is the e-fuels. They are produce from electricity and CO_2, and are considered a promising sustainable fuel source to replace fossil fuels (König et al., 2019). However, their lifecycle greenhouse gas emissions are conditioned by the electricity source used for its production.

4. Conclusions

In this work, a laser induced plasma ignition system was successfully applied to assist ignition of low-reactivity fuels, like diesel-gasoline blends, in an optically accessible compression ignition engine. The main conclusions that can be extracted are:

- When LIP forces an ignition delay of the blends similar to pure diesel, their combustion is also very similar and so it does the energy released, independently of the amount of gasoline in the blend.
- Small differences were observed in terms of energy release between diesel and blends, when ignition is forced by LIP. However, an increase of in-cylinder temperature reduces them, which suggest that the combustion process could still be affected by fuel composition.
- An increase of the gasoline content in the blend reduces soot formation, even when a shorter lift-off length is forced by LIP.

- Results confirm the capability of the LIP to change not only the ignition delay but also the flame lift-off length, which is strongly related with soot formation.
- It has been proved that the LIP ignition system allows to reduce particle matter formation and improve combustion efficiency. However, the fuels used still play a major role in terms of CO_2 emissions. Sustainable fuels, like biofuels or renewable e-fuels, could provide a global CO_2 mitigation if the whole lifecycle is considered.

Acknowledgements

The authors acknowledge that this research work has been partly funded by the Government of Spain and FEDER under TRANCO project (TRA2017-87694-R).

5. Bibliography

Ahmed, W., Sarkar, B., 2018. Impact of carbon emissions in a sustainable supply chain management for a second generation biofuel. J. Clean. Prod. 186, 807–820. https://doi.org/10.1016/j.jclepro.2018.02.289

AlAbbad, M., Aljohani, K., Farooq, A., 2019. Ignition delay measurements of diesel and gasoline blends, in: 12th Asia-Pacific Conference on Combustion, ASPACC 2019.

Bae, C., Kim, J., 2017. Alternative fuels for internal combustion engines. Proc. Combust. Inst. https://doi.org/10.1016/j.proci.2016.09.009

Bakker, P.C., Maes, N., Dam, N., 2017. The potential of on- and off-resonant formaldehyde imaging combined with bootstrapping in diesel sprays. Combust. Flame 182, 20–27. https://doi.org/10.1016/j.combustflame.2017.03.032

Barrientos, E.J., Lapuerta, M., Boehman, A.L., 2013. Group additivity in soot formation for the example of C-5 oxygenated hydrocarbon fuels. Combust. Flame 160, 1484–1498. https://doi.org/10.1016/j.combustflame.2013.02.024

Benajes, J., García, A., Domenech, V., Durrett, R., 2013. An investigation of partially premixed compression ignition combustion using gasoline and spark assistance. Appl. Therm. Eng. 52, 468–477. https://doi.org/10.1016/j.applthermaleng.2012.12.025

Benajes, J., García, A., Monsalve-Serrano, J., Boronat, V., 2017. Achieving clean and efficient engine operation up to full load by combining optimized RCCI and dual-fuel diesel-gasoline combustion strategies. Energy Convers. Manag. 136, 142–151. https://doi.org/https://doi.org/10.1016/j.enconman.2017.01.010

Bermúdez, V., García, J.M., Juliá, E., Martínez, S., 2003. Engine with optically accessible cylinder head: A research tool for injection and combustion processes. SAE Tech. Pap. https://doi.org/10.4271/2003-01-1110

Dale, J.D., Smy, P.R., Clements, R.M., 1978. Laser ignited internal combustion engine - An experimental study. SAE Tech. Pap. https://doi.org/10.4271/780329

Felix Jiri Weinberg, J.R.W., 1971. A preliminary investigation of the use of focused laser beams for minimum ignition energy studies. Proc. R. Soc. London. A. Math. Phys. Sci. 321, 41–52. https://doi.org/10.1098/rspa.1971.0012

Genzale, C.L., Pickett, L.M., Hoops, A.A., Headrick, J.M., 2011. Laser ignition of multi-injection gasoline sprays. SAE 2011 World Congr. Exhib. https://doi.org/10.4271/2011-01-0659

Gómez, A., García-Contreras, R., Soriano, J.A., Mata, C., 2020. Comparative study of the opacity tendency of alternative diesel fuels blended with gasoline. Fuel 264, 116860. https://doi.org/10.1016/J.FUEL.2019.116860

Goto, S., Lee, D., Wakao, Y., Honma, H., Mori, M., Akasaka, Y., Hashimoto, K., Motohashi, M., Konno, M., 1999. Development of an LPG DI Diesel Engine Using Cetane Number Enhancing Additives, in: International Fuels & Lubricants Meeting & Exposition. SAE International. https://doi.org/https://doi.org/10.4271/1999-01-3602

Han, D., Wang, C., Duan, Y., Tian, Z., Huang, Z., 2014. An experimental study of injection and spray characteristics of diesel and gasoline blends on a common rail injection system. Energy 75, 513–519. https://doi.org/https://doi.org/10.1016/j.energy.2014.08.006

Higgins, B., Siebers, D., 2001. Measurement of the flame lift-off location on di diesel sprays using OH chemiluminescence. SAE Tech. Pap. https://doi.org/10.4271/2001-01-0918

Hossain, A.., Davies, P.., 2010. Plant oils as fuels for compression ignition engines: A technical review and life-cycle analysis. Renew. Energy. https://doi.org/10.1016/j.renene.2009.05.009

Hu, Y., Wang, Z., Li, X., 2020. Impact of policies on electric vehicle diffusion: An evolutionary game of small world network analysis. J. Clean. Prod. 265. https://doi.org/10.1016/j.jclepro.2020.121703

Hwang, J., Kim, W., Bae, C., Choe, W., Cha, J., Woo, S., 2017. Application of a novel microwave-assisted plasma ignition system in a direct injection gasoline engine. Appl. Energy 205, 562–576. https://doi.org/10.1016/j.apenergy.2017.07.129

Jian, D., Xiaohong, G., Gesheng, L., Xintang, Z., 2001. Study on Diesel-LPG Dual Fuel Engines, in: SAE International Fall Fuels & Lubricants Meeting & Exhibition. SAE International. https://doi.org/https://doi.org/10.4271/2001-01-3679

Kim, H., Choi, B., 2008. Effect of ethanol–diesel blend fuels on emission and particle size distribution in a common-rail direct injection diesel engine with warm-up catalytic converter. Renew. Energy 33, 2222–2228. https://doi.org/10.1016/J.RENENE.2008.01.002

König, A., Ulonska, K., Mitsos, A., Viell, J., 2019. Optimal Applications and Combinations of Renewable Fuel Production from Biomass and Electricity. Energy and Fuels 33, 1659–1672. https://doi.org/10.1021/acs.energyfuels.8b03790

Kumar, S., Cho, J.H., Park, J., Moon, I., 2013. Advances in diesel-alcohol blends and their effects on the performance and emissions of diesel engines. Renew. Sustain. Energy Rev. 22, 46–72. https://doi.org/10.1016/j.rser.2013.01.017

Liu, F., Gao, Y., Wu, H., Zhang, Z., He, X., Li, X., 2018. Investigation on Soot Characteristics of Gasoline/Diesel Blends in a Laminar Coflow Diffusion Flame. Energy and Fuels 32, 7841–7850. https://doi.org/10.1021/acs.energyfuels.7b04051

Liu, H., Wang, Z., Li, Y., Zheng, Y., He, T., Wang, J., 2019. Recent progress in the application in compression ignition engines and the synthesis technologies of polyoxymethylene dimethyl ethers. Appl. Energy. https://doi.org/10.1016/j.apenergy.2018.10.064

Medeiros, D.L., Sales, E.A., Kiperstok, A., 2015. Energy production from microalgae biomass: Carbon footprint and energy balance. J. Clean. Prod. 96, 493–500. https://doi.org/10.1016/j.jclepro.2014.07.038

Miller Jothi, N.K., Nagarajan, G., Renganarayanan, S., 2007. Experimental studies on homogeneous charge CI engine fueled with LPG using DEE as an ignition enhancer. Renew. Energy 32, 1581–1593. https://doi.org/10.1016/J.RENENE.2006.08.007

Nerva, J., 2013. An assessment of fuel physical and chemical properties in the combustion of a Diesel spray. Universitat Politècnica de València.

Omari, A., Heuser, B., Pischinger, S., 2017. Potential of oxymethylenether-diesel blends for ultra-low emission engines. Fuel 209, 232–237. https://doi.org/10.1016/j.fuel.2017.07.107

Pastor, J., Garcia-Oliver, J.M., Garcia, A., Nareddy, V.R., 2017. Characterization of Spray Evaporation and Mixing Using Blends of Commercial Gasoline and Diesel Fuels in Engine-Like Conditions. SAE Tech. Pap. Ser. 1. https://doi.org/10.4271/2017-01-0843

Pastor, J.M.J.V., Javier López, J., García, J.M., Pastor, J.M.J.V., 2008. A 1D model for the description of mixing-controlled inert diesel sprays. Fuel 87, 2871–2885. https://doi.org/10.1016/j.fuel.2008.04.017

Pastor, J.V., Garcia-Oliver, J.M., Novella, R., Xuan, T., 2015. Soot Quantification of Single-Hole Diesel Sprays by Means of Extinction Imaging. SAE Int. J. Engines 8. https://doi.org/10.4271/2015-24-2417

Pastor, J.V., García, A., Micó, C., Lewiski, F., 2020. An optical investigation of Fischer-

Tropsch diesel and Oxymethylene dimethyl ether impact on combustion process for CI engines. Appl. Energy 260. https://doi.org/10.1016/j.apenergy.2019.114238

Pastor, J. V., García-Oliver, J.M., García, A., Micó, C., Durrett, R., 2013. A spectroscopy study of gasoline partially premixed compression ignition spark assisted combustion. Appl. Energy 104, 568–575. https://doi.org/10.1016/j.apenergy.2012.11.030

Pastor, J. V., García-Oliver, J.M., García, A., Micó, C., Möller, S., 2016a. Application of optical diagnostics to the quantification of soot in n-alkane flames under diesel conditions. Combust. Flame 164, 212–223. https://doi.org/10.1016/J.COMBUSTFLAME.2015.11.018

Pastor, J. V., García-Oliver, J.M., García, A., Pinotti, M., 2017. Effect of laser induced plasma ignition timing and location on Diesel spray combustion. Energy Convers. Manag. 133, 41–55. https://doi.org/10.1016/j.enconman.2016.11.054

Pastor, J. V., García-Oliver, J.M., García, A., Pinotti, M., 2016b. Laser induced plasma methodology for ignition control in direct injection sprays. Energy Convers. Manag. 120, 144–156. https://doi.org/10.1016/j.enconman.2016.04.086

Pastor, J. V., García-Oliver, J.M., Pastor, J.M., Vera-Tudela, W., 2015. One-dimensional diesel spray modeling of multicomponent fuels. At. Sprays 25, 485–517. https://doi.org/10.1615/AtomizSpr.2014010370

Pastor, José V., García, A., Micó, C., García-Carrero, A.A., 2020. Experimental study of influence of Liquefied Petroleum Gas addition in Hydrotreated Vegetable Oil fuel on ignition delay, flame lift off length and soot emission under diesel-like conditions. Fuel 260, 116377. https://doi.org/10.1016/J.FUEL.2019.116377

Phuoc, T.X., 2006. Laser-induced spark ignition fundamental and applications. Opt. Lasers Eng. 44, 351–397. https://doi.org/10.1016/J.OPTLASENG.2005.03.008

Pickett, L.M., Siebers, D.L., 2004. Soot in diesel fuel jets: effects of ambient temperature, ambient density, and injection pressure. Combust. Flame 138, 114–135. https://doi.org/10.1016/J.COMBUSTFLAME.2004.04.006

Rajak, U., Nashine, P., Verma, T.N., 2020. Effect of spirulina microalgae biodiesel enriched with diesel fuel on performance and emission characteristics of CI engine. Fuel 268. https://doi.org/10.1016/j.fuel.2020.117305

Sequino, L., Mancaruso, E., Monsalve-Serrano, J., Garcia, A., 2020. Infrared/Visible Optical Diagnostics of RCCI Combustion with Dieseline in a Compression Ignition Engine, in: SAE Technical Papers. https://doi.org/10.4271/2020-01-0557

Triantopoulos, V., Martz, J.B., Sterniak, J., Lavoie, G., Assanis, D.N., Bohac, S.V., 2020. Operating limits of spark-assisted compression ignition combustion under boosted ultra-EGR dilute conditions in a negative valve overlap engine, in: ASME 2019 Internal Combustion Engine Division Fall Technical Conference, ICEF 2019. https://doi.org/10.1115/ICEF2019-7220

Vu, D.N., Das, S.K., Jwa, K., Lim, O., 2019. Characteristics of auto-ignition in gasoline–biodiesel blended fuel under engine-like conditions. Proc. Inst. Mech. Eng. Part D

J. Automob. Eng. 233, 1352–1364. https://doi.org/10.1177/0954407018763194

Wang, C., Wood, J., Wang, Y., Geng, X., Long, X., 2020. CO<inf>2</inf> emission in transportation sector across 51 countries along the Belt and Road from 2000 to 2014. J. Clean. Prod. 266. https://doi.org/10.1016/j.jclepro.2020.122000

Wang, J., Yang, F., Ouyang, M., 2015. Dieseline fueled flexible fuel compression ignition engine control based on in-cylinder pressure sensor. Appl. Energy 159, 87–96. https://doi.org/10.1016/j.apenergy.2015.08.101

Weinrotter, M., Wintner, E., Iskra, K., Neger, T., Olofsson, J., Seyfried, H., Dén, M., Lackner, M., Winter, F., Vressner, A., Hultqvist, A., Johansson, B., 2005. Optical diagnostics of laser-induced and spark plug-assisted hcci combustion. SAE Tech. Pap. https://doi.org/10.4271/2005-01-0129

Westlye, F.R., Penney, K., Ivarsson, A., Pickett, L.M., Manin, J., Skeen, S.A., 2017. Diffuse back-illumination setup for high temporally resolved extinction imaging. Appl. Opt. 56, 5028–5038. https://doi.org/10.1364/AO.56.005028

Xuan, T., Desantes, J.M., Pastor, J.V., Garcia-Oliver, J.M., 2019. Soot temperature characterization of spray a flames by combined extinction and radiation methodology. Combust. Flame 204, 290–303. https://doi.org/10.1016/j.combustflame.2019.03.023

Xuan, Tiemin, Pastor, J. V., García-Oliver, J.M., García, A., He, Z., Wang, Q., Reyes, M., 2019. In-flame soot quantification of diesel sprays under sooting/non-sooting critical conditions in an optical engine. Appl. Therm. Eng. 149, 1–10. https://doi.org/10.1016/J.APPLTHERMALENG.2018.11.112

Yan, X., Corbin, K.R., Burton, R.A., Tan, D.K.Y., 2020. Agave: A promising feedstock for biofuels in the water-energy-food-environment (WEFE) nexus. J. Clean. Prod. 261. https://doi.org/10.1016/j.jclepro.2020.121283

Yilmaz, N., Vigil, F.M., Burl Donaldson, A., Darabseh, T., 2014. Investigation of CI engine emissions in biodiesel–ethanol–diesel blends as a function of ethanol concentration. Fuel 115, 790–793. https://doi.org/10.1016/J.FUEL.2013.08.012

Zheng, L., Ma, X., Wang, Z., Wang, J., 2015. An optical study on liquid-phase penetration, flame lift-off location and soot volume fraction distribution of gasoline–diesel blends in a constant volume vessel. Fuel 139, 365–373. https://doi.org/10.1016/J.FUEL.2014.09.009

Nomenclature

ICE: Internal Combustion Engines

CI: Compression Ignition

SI: Spark ignition

LTC: Low Temperature Combustion

SACI: Spark Assisted Compression Ignition

LIP: Laser induced plasma

LRF: Low-Reactivity Fuel

TDC: Top Dead Center

CAD: crank angle degree

LT: Low Temperature

MT: Medium Temperature

HT: High Temperature

T_{cyl} = In-cylinder temperature around top dead center

P_{inj} = Injection pressure

ID: Ignition Delay

SoE: Start of Energizing

aSoE: After Start of Energizing

aSoI: After Start of Energizing

aHR: Apparent Heat Released

aRoHR: Apparent Rate of Heat Released

$\dot{m}f$: mass flow rate

mf_{cc}: Total mass of fuel injected per cylinder and cycle

H_c: Lower heating value

ϕ_{LOL}: fuel-air equivalence ratio at Lift-off Length

NL: Natural Luminosity

DBI: Diffused Back Illumination

LOL: Lift-off Length

7030: 70% gasoline – 30% diesel

5050: 50% gasoline – 50% diesel

B0: 100% diesel

KL: Soot optical density

SP: Smoke Point

TSI: Threshold Sooting Index

OESI: Oxygen Extended Sooting Index